Research Square

Preprints are preliminary reports that have not undergone peer review.
They should not be considered conclusive, used to inform clinical practice,
or referenced by the media as validated information.

Earliest Iron Blooms Discovered off the Carmel Coast Revise Mediterranean Trade in Raw Metal ca. 600 BCE

Tzilla Eshel

teshel@univ.haifa.ac.il

University of Haifa

Andrei Ioffe

Technion – Israel Institute of Technology

Dafna Langgut

Tel Aviv University

Yoav Bornstein

University of Haifa

Zachary C. Dunseth

University of California San Diego

Marko Runjajić

University of Haifa

Shmuel Ariely

Technion – Israel Institute of Technology

Thomas E. Levy

University of California San Diego

Assaf Yasur-Landau

University of Haifa

Article

Keywords:

Posted Date: December 10th, 2025

DOI: https://doi.org/10.21203/rs.3.rs-8281730/v1

License: This work is licensed under a Creative Commons Attribution 4.0 International License. Read Full License

Additional Declarations: No competing interests reported.

Version of Record: A version of this preprint was published at npj Heritage Science on March 13th, 2026. See the published version at https://doi.org/10.1038/s40494-026-02409-7.

Abstract

The discovery of exceptionally well-preserved iron blooms during underwater excavations at the Dor Lagoon provides a rare and transformative window into southern Levantine Iron Age metallurgy and trade following the collapse of Late Bronze Age civilizations in the eastern Mediterranean. For the first time, unworked iron blooms, still encased in protective slag, have been recovered, representing the earliest securely dated form of industrial iron products in the archaeological record, to date. Radiocarbon modeling of an embedded charred oak twig, together with additional short-lived carbon samples, dates the blooms to the late 7th to early 6th centuries BCE.

These findings challenge long-standing assumptions that iron blooms were typically forged into billets or bars immediately after smelting, and question suggestions that iron smelting took place within southern Levantine urban centers. Instead, the Dor blooms demonstrate that raw iron was transported in its as-smelted state across the Mediterranean, with adhering slag layers protecting the metal from corrosion during shipment. This pattern suggests that Iron Age urban centers concentrated on smithing rather than smelting activities. The finds further indicate that raw iron was circulating as a traded commodity, possibly under Egyptian rule following the Neo-Assyrian withdrawal from the region, opening new commercial networks, particularly with the Aegean.

Introduction

Iron is the most abundant heavy metal on earth's crust, yet humans learned how to produce it thousands of years after the introduction of copper, bronze, silver and gold. This is probably due to its unique production method in premodern times, known as the bloomery process, or smelting, which involved heating the ore in a furnace with carbon-rich fuel at temperatures of approximately 1200°C. Unlike other metals, the iron did not melt during this process. Instead, the reduction of iron oxides resulted in the slow formation of a solid mass of metal, known as a "bloom." As the bloom formed, particles of slag and charcoal became embedded within it. To remove the adhering slag and expel these inclusions, primary smithing was performed by hammering the bloom, typically while it was still hot (1–6). Simultaneously, this also consolidated the metal into a more compact and manageable billet or bar, which could be further worked to produce iron tools—a process termed "secondary smithing" (7). The bloomery process was assumed to be the state of technology from the Iron Age (ca. 10th century BCE) to the Umayyad period (7th–8th centuries CE) and possibly later (8–9).

The reasons for the transition from bronze to iron are not fully known. Possible explanations are easier access to the mining sources of iron, in place of copper and tin, the main components of bronze; and/or superior properties of iron/steel compared to bronze. These properties may have been provided by the mastery of technological steps, which involved alloying carbon with iron (transforming it into steel) and applying thermal treatment—two techniques that make iron harder than bronze. Alternatively, they may have been the natural outcome of uncontrolled smelting operations that created blooms, a mixture of iron/steel (e.g., 10).

Once metalsmiths mastered this technology, iron became a valuable resource, widely used to manufacture various tools, weapons, and other objects. Societies relied heavily on iron for agriculture, manufacturing, construction, shipbuilding, and military activities, making it a strategic resource. However, the production and

utilization of iron and steel, from raw ore to finished tools, were constrained by geological and environmental factors. In the Levant, local iron ore deposits were notably scarce. Limited quantities of iron oxides were found in the Jordan Rift Valley (11–12), where iron production was recently reviewed (9, 13). Consequently, since the onset of the Iron Age, much of the iron required for both civilian and military purposes in the southern Levant was probably imported, necessitating political agreements and commercial alliances to secure supplies (14).

Extractive iron metallurgy originated in Anatolia in the early Iron Age, yet the first to adopt this technology broadly were the Levantines and Cypriots (4, 15–16). The importance of the Levant in the expansion of iron metallurgy during the Iron IIA (~ 950–800 BCE) has been established based on well-documented ironworking debris (10, 17–20). Evidence of ironworking in the Levant is found in contexts dating from the Iron Age to the Persian period (21–25). Maritime trade, driven by the Phoenicians, probably played a continuing key role in spreading iron technologies across the Mediterranean throughout these periods (26–31).

Iron was customarily transported in the form of billets and bars, which were produced by working and forging blooms, and are known to have been produced since the Iron Age. Some examples were found at sites in the territory of the 8th-century BCE Neo-Assyrian Empire (4). Numerous finds of billets and bars across Europe indicate that these were the preferred forms for inland transportation of iron since the 7th century BCE (4, 32–33). Starting from the Hellenistic period, there is evidence that they were shipped across the Mediterranean, with the earliest underwater example being the corroded iron billets from the late-3rd-century BCE Kyrenia shipwreck (34). On the basis of these finds, it is widely accepted that iron was traded and imported as semi-finished or finished products (e.g., 10).

Blooms, in contrast, are a rare and unexpected find prior to the Roman Period. In Europe, over 500 blooms or bloom fragments from 90 sites were recorded, but only 13 could be securely attributed to pre-Roman contexts (Hallstatt period, Iron Age, roughly 8th–6th centuries BCE; 3). In the Levant, the only evidence of whole blooms is from the Carmel Coast. Exposed by a storm, 93 partly consolidated blooms were revealed, alongside nails and different types of iron bars. The finds, however, were dated by the excavators to the 12th century AD (35). It was thus assumed that early smiths tended to “strike while the iron was hot,” processing the blooms to billets immediately after smelting, explaining the scarcity of unworked or intact blooms in earlier contexts.

Therefore, iron masses yielded in a cargo revealed in the recent underwater excavations of the Dor Lagoon, south of Tel Dor (Fig. 1), are a unique find. The cargo, termed Dor L, lay at a shallow depth of about 3 m below sea level. In addition to the iron masses, it included basket-handle amphorae, some with resin-coated interiors; a composite lead-and-wood anchor; and ballast stones. Pottery typology and radiocarbon dates of short-lived samples date the cargo to the 7th–6th centuries BCE (36).

Following the excavations, one of the masses was sectioned and subjected to microscopic, chemical and radiocarbon analyses. The results, as we demonstrate below, indicate that it was an unworked iron bloom from the late 7th or early 6th centuries BCE. The finds therefore challenge previous assumptions regarding maritime trade of iron and provide the missing link in the *chaîne opératoire* of iron production and transportation during the Iron Age.

Materials

Nine sub-rectangular heavy blooms were unearthed in the Dor Lagoon (Fig. 1). Their weight ranges between 5–10 kilograms, and their average size is 17 × 14 × 11 cm (Table S1). Their outer surface is covered with light concretions, including sand and shells of bivalves, consistent with the makeup of the sediment in which they rested. An initial chemical composition of one of the items (Fig. S1:3; Table S1:3) was measured in an exposed area of the metal, using an Olympus Vanta M Series XRF. The results show that the item was made of iron. This bloom was selected for further examination, to gain additional insights into these items and understand their function.

Methods

Conservation procedure

Iron is highly vulnerable to corrosive processes, especially when extracted from seawater, which is rich in chloride. Once the surface of the iron is exposed, residual chloride ions migrate through pores in the metal and cause corrosion in the entire item (37). This necessitates a desalination process, through which the chloride is gradually removed without damaging the blooms. A silver nitrate chloride test was used to measure the relative amount of chlorides released from the bloom (38).

Metallurgical analyses

A cross-section was extracted from one iron bloom (Fig. 2) using a metallographic cutting machine. The section was further cut into smaller sections representing the sides and the core of the cross-section, denoted samples S-I and S-II (Fig. 2b).

The microstructures of samples S-I and S-II were analyzed after mounting in Bakelite, followed by grinding and polishing. Optical microscopy (OM) was performed using an Olympus BX51 light microscope while SEM was conducted with a Thermo Fisher Prisma equipped with Oxford energy dispersion spectroscopy (EDS) and wavelength dispersion spectroscopy (WDS) detectors applied for analysis of the composition of slags and corrosion products. A Zeiss Ultra-Plus High Resolution-SEM equipped with a Bruker electron backscattered diffraction (EBSD) detector and a Rigaku SmartLab X-ray diffractometer was used for phase analysis. The hardness of the samples was measured using a Micro Vickers Future Tech tester with a 100-gram load.

Commonly used chemical analysis methods providing information about the average composition of the sample's area on a scale of centimeters could not be applied to determine the base metal composition, due to the presence of several pores, many of which contained slag inclusions and corrosion products. The presence of slag could have led to errors in the results. Therefore, a scanning electron microscope equipped with a WDS detector with a higher sensitivity was used to estimate the base metal composition, including trace elements.

Corrosion products on the sample surface and inside pores were examined using XRD and EBSD.

The metallurgical analyses were performed at the Israel Institute of Materials Manufacturing Technology (IMT).

Dendroarchaeological analysis of charred wood

A small, charred wood fragment embedded within the iron bloom was subjected to dendroarchaeological analysis and radiocarbon dating. Taxonomic identification of the charred sample was carried out by examining the wood's anatomical structure with the use of a Carl Zeiss SteREO Discovery.V20 microscope. Anatomical determination was based on comparison with a wood and charcoal reference collection (the Steinhardt Museum of Natural History), as well as published wood anatomy atlases (39–42).

Radiocarbon modeling

To narrow down the historical context of this unique find, radiocarbon dates of short-lived samples obtained from the Dor L2 cargo (36) were remodeled. Together with the pottery found on the boat, the cargo was given a chronological range of about 700–530 BCE (Iron IIC). In this study, we model the radiocarbon ages from the short-lived samples to better determine the lower chronological boundary of the cargo. The goal is to understand whether the lower date range for the cargo includes also the Persian period (beginning at Dor ca. 525 BCE) or ends before it, during the Babylonian period. To do so, we estimate the date of the ship's last voyage (LV) following the shipwreck methodology outlined in Manning et al. (43). Briefly, this Oxcal phase model uses a Tau Boundary paired with a Boundary, which assumes that the dates in the assemblage are more likely toward the end of the lifespan of the phase—in this case, the sinking of the ship (43–45).

We intentionally selected the twig from the iron bloom, along with radiocarbon samples that relate to wine and its transportation, specifically, grape seeds and resin from amphorae— in this case, the cargo with the shortest shelf life. Historical documents indicate that wine was usually intended for consumption within one to two years of production (see 46 and references therein). For example, the Ahiqar scroll, an erased customs account (dated to 475 or 454 BCE), records only vintages of two specific years (years 10 and 11, interpreted as referring to the reign of Xerxes) (47). Twentieth-century CE ethnographic accounts from Greece also attest to usual consumption within one to two years (e.g., 48). We therefore produced models where the ship's LV is constrained by a uniform distribution of a maximum of + 3, + 5, + 10, + 20 years (+ 10 and + 20 years to account for the possibility of very old aged wine) after the production of the wine and/or preparation of the wine storage vessels.

Results

Conservation procedure

The blooms were placed in tap water for five months and the water was changed every four weeks. For some of the blooms (nos. 1, 2, 4, and 5), sodium carbonate was added to the water to increase the pH and reduce possible corrosion. After five months, a silver nitrate chloride test revealed that the amount of chlorides

released in 24 hours was less than 10 ppm. At that point, the blooms were removed from the tap-water baths, air-dried, and stored in a dry cabinet with a relative humidity of 20%.

Metallurgical analyses

Samples S-I and S-II–obtained from the surface and bulk of the bloom's cross-section respectively–were selected for further analysis (Fig. 2b).

Optical microscopy (OM)

The microstructure of the surface of the iron bloom (Sample S-I) revealed that it is covered with a crust of slag and postdepositional deposits, with a total thickness of 2–4 mm, comprising two layers divided into several phases (Fig. 3a).

The macrostructure of the bulk of the iron bloom (Sample S-II) contains numerous pores and inclusions of different sizes, from several millimeters to several microns. The microstructure of this sample shows iron with varying carbon contents. It presents relatively coarse ferrite and pearlite grains, yet the share of perlite varies across the sample. In some areas, nearly pure iron is evident (Fig. 3b, c), while in other regions a larger share of perlite with acicular ferrite can be seen. Note also the Widmanstätten structure, which indicates relatively rapid cooling (49; Fig. 3d). Such microstructure is typical of iron with a nonhomogeneous carbon content resulting from the iron being cooled from an austenitic state at a rapid and uncontrolled cooling rate.

Hardness

Vickers hardness was measured at 16 random points across the cross-section. Due to different microstructures, the hardness of the metal ranges widely from 73 to 129 $HV_{0.5}$, with a mean value of 103 HV_{05}.

Base metal composition (measured with WDS)

The base metal composition was analyzed within micron locality and averaged using WDS. Results indicate traces of Si (0.02 wt%), Ni (0.11 wt%), S (0.01 wt.%) and P (0.01 wt.%) (Tables S2, S3 and Fig. S2). Although carbon content cannot be measured with WDS, OM images (Fig. 3) suggest that the base metal contains low amounts of carbon. The results show traces of nickel and low concentrations of sulfur and phosphorus, indicating nearly pure iron.

SEM-EDS analysis

The microstructure and composition of the bloom's crust (Sample S-I) were further analyzed using SEM-EDS (Figs. 4a, S2; Table 1).

Table 1
Composition of particles (EDS), shown in Fig. 4 [At %].

Fig.	Label	O	Mg	Al	Si	P	S	Cl	K	Ca	Ti	Fe	Zn
4a	1 (Sand)	71.7	0.0	0.0	28.2	0.0	0.0	0.0	0.0	0.0	0.0	0.1	0.0
	2 (Ca-containing sediments)	70.2	5.8	0.1	8.5	0.0	0.2	0.6	0.0	11.1	0.0	3.5	0.0
	3 (S-containing sediments and corrosion products)	36.2	0.4	0.2	0.2	0.0	22.7	0.0	0.0	0.0	0.0	40.2	0.0
	4 (S-containing sediments and corrosion products)	9.0	0.4	0.0	1.0	0.1	44.6	0.0	0.0	0.1	0.0	44.9	0.0
	5 (Mg-containing sediments)	57.1	12.8	0.3	11.1	0.1	6.7	0.5	0.0	2.1	0.0	9.4	0.0
	6 (FeO-containing products)	51.1	0.3	0.4	0.2	0.0	2.9	0.0	0.0	0.0	0.0	45.2	0.0
	7 (FeO-containing products)	56.2	0.3	0.1	1.0	0.0	0.2	0.1	0.0	0.1	0.0	42.1	0.0
	8 (slag, glass)	60.2	0.4	5.5	14.6	0.3	0.2	0.0	1.1	7.7	0.1	10.0	0.1
	9 (slag, FeO)	48.4	0.4	1.9	3.7	0.1	0.1	0.4	0.2	1.6	0.1	43.1	0.0
	10 (slag, iron)	0.0	0.0	0.1	0.1	0.0	0.0	0.0	0.0	0.0	0.0	99.8	0.0
4b	1 (iron)	0.0	0.0	0.0	0.1	0.0	0.0	0.0	0.0	0.0	0.0	99.9	0.0
	2 (FeO)	49.4	0.4	0.5	0.2	0.0	0.0	0.0	0.0	0.1	0.2	49.2	0.1
	3 (glassy slag)	58.6	0.4	5.4	14.3	0.2	0.1	0.1	1.0	8.4	0.1	11.3	0.1
4c	1 FeO	48.7	0.4	0.6	0.4	0.0	0.0	n.d.	0.0	0.1	0.1	0.1	49.6
	2 Glassy slag	60.0	0.4	5.7	15.5	0.2	0.1	n.d.	1.0	6.4	0.0	0.0	10.4

The results reveal that the crust contains two layers: an external, postdepositional layer, formed under the sea, and an underlying layer, as detailed below:

1. Postdepositional layer: The crust's external layer consists of deposits that were formed during the bloom's exposure to seawater. Three different postdepositional phases were distinguished in these deposits:

1.1. The outermost phase of the deposits was enriched in S, Mg, and Ca, typically formed in the sea by biomineralization processes (50–51).

1.2. In the middle phase, particles enriched with Si and O were indicated. The Si:O atomic ratio suggests these particles may have been embedded with sand.

1.3. The innermost phase consists of corrosion products, including enriched particles of Fe, S, and O. These are formed as a reaction of iron and slag with seawater. Fe- and O-containing particles are a mixture of iron oxides and hydroxides, which are typical corrosion products of iron in mineralized water. The presence of iron sulfides can be explained by microbiologically influenced corrosion (MIC).

Almost no chlorides are present on the exterior of the sample (Fig. S2, Table 1), probably because soluble chlorides were washed away during the desalination process in the laboratory (see above); however, a small amount of chlorine is found under the deposits on the interface with the slag.

2. Underlying glassy layer. A glassy phase, which is a solid solution of several oxides, mostly Al, Si, Ca, and K, and traces of Mg, Ti, P, S, and Zn, is evident all around the bloom, under the postdepositional deposits (Fig. 4a; Table 1).

Iron oxide particles with a diameter of 10–100 μm, shaped like fused clustered ellipsoids, were identified in the slag's glass (Fig. 4b). The chemical composition of these particles shows an Fe:O ratio of 1:1, suggesting that they are wüstite. These particles are therefore identified as fragments of iron ore that were used during smelting. Their transformation into iron due to reduction by CO during smelting is presented in Fig. 4b.

Slag inclusions, similar in composition and microstructure to those on the bloom's surface, are present inside the iron bloom (Fig. 4c, Table 1). This further confirms that the layer covering the bloom's surface originated in the smelting furnace. This is a rare case in which the smelting crust–which formed during the smelting process–was not removed and is still present.

Many pores were detected in the iron bloom. The pores show no signs of closing or deformation (Figs. 2, 3). Their morphology closely resembles clustered ellipsoids. Fine features formed during ferrite grain growth and pearlite grain growth are visible on the surfaces of the pores (see Fig. S3). These features could be formed only at the cooling stage of the bloom during smelting, with no additional processing. The absence of deformation suggests that the iron bloom was neither forged nor mechanically processed after smelting and cooling. Additional analysis of the pores is available in SI.

Dendroarchaeological and radiocarbon analysis of charred wood

The small piece of charcoal, which was likely trapped within the ingot during the blooming process, was identified as oak (*Quercus* sp.) (Fig. 5a, b; see more in SI). It was determined to be of relatively young age or from a younger portion of the plant, based on its ring curvature. The charcoal was identified by the rays of two

different sizes (uniseriate rays and very large rays), diffuse-in-aggregate parenchyma, and mostly solitary vessels, especially away from the ring boundary. The vessels were ring-porous (with a maximum diameter at the ring boundary of ca. 75 µm), indicating a deciduous oak type. Oaks can make for good smelting and metalworking fuels, due to their thick fibers. The latter contribute to their high wood densities and consequent high calorific values, potentially making them hotter and longer burning fuels than other available wood types (e.g., 42, 52).

A fragment of a young branch of deciduous oak was subjected to AMS ^{14}C measurement and yielded, upon calibration, an age range in the 2σ interval from 770 to 540 cal. BCE (36). The identification of the branch as young minimized the old wood effect, increasing the accuracy of the analysis.

Radiocarbon modelling

The LV models were produced using Oxcal 4.4.4 (53) and the IntCal20 calibration curves (54) and are presented in Fig. 5c and Table 2. The Oxcal code is available in SI. Note that, since the wooden hull from the wreck did not survive, we cannot constrain the date range further by dating the felling of trees used for construction, or other objects (dunnage, etc.), from the lifetime of the ship (as outlined in 43). Therefore, we selected the short-lived samples that relate to wine, a commodity with short shelf life compared to boat timber, to provide a stronger indication for the chronology of the LV. All models produced a median date around 639–631 BCE and a range of dates from approximately the mid-8th to mid-6th centuries BCE, all before 536 BCE, and thus preclude the Persian period as a possible date for the cargo.

Table 2
Modeled date ranges for Last Voyage. Models are available in Figures S6–S9.

	+ 3 yrs		+ 5 yrs		+ 10 yrs		+ 20 yrs	
	1 σ (68.3%)	2 σ (95.4%)	1 σ (68.3%)	2 σ (95.4%)	1 σ (68.3%)	2 σ (95.4%)	1 σ (68.3%)	2 σ (95.4%)
LV date range	750–545 BCE	754–542 BCE	749–544 BCE	753–541 BCE	747–543 BCE	752–538 BCE	743–541 BCE	749–536 BCE
LV median	639 BCE		638 BCE		635 BCE		631 BCE	

Discussion

The nine iron blooms discovered in the Dor Lagoon, dating between the late 7th and early 6th centuries BCE, constitute the earliest securely dated assemblage of multiple iron blooms known to date. While an earlier isolated bloom has been reported from a Kyjatice-culture pit at Šafárikovo (Hallstatt B3 period, ca. 8th century BCE) in southern Slovakia (55–56), this exceptional find remains singular and is equivalent in size to the average blooms of much later periods (3). Most other archaeologically documented iron blooms are significantly later in date, yielded in post-Iron Age contexts (3). The Dor assemblage, therefore, provides unique and unprecedented insight into early bloom production, handling, and maritime transport during the Iron Age.

Technological implications

These findings introduce a new class of Iron Age iron products—whole unworked iron blooms—previously undocumented in the archaeological record of the Levant. The metallurgical analysis of one bloom reveals solid, well-preserved, low-carbon iron with a ferrite-perlite microstructure and an average hardness of ~ 100 HV. Numerous slag inclusions and pores are present, none of which show deformation from forging, confirming that the bloom remains in its original as-smelted state.

A glassy slag crust was identified beneath the marine concretions on the bloom surface, containing fragments of iron ore and matching the composition of internal slag inclusions. This suggests the bloom was transported wrapped in slag—a highly unexpected observation, as slag was typically removed during hot hammering to consolidate the bloom (17). The slag layer likely provided protection against corrosion, explaining the exceptional preservation of the metallic iron after 2,600 years underwater. These findings demonstrate that shipping blooms in their as-smelted, slag-encased state was an effective and economical method of long-distance transport (see more below).

The low-carbon blooms are inferior in comparison to cold-hammered and annealed bronze. The mechanical properties of iron—its hardness and tensile strength, in particular—are not inherent characteristics of the material condition of the metal. They are provided solely by the mastery of specific production steps that add carbon to the iron, which significantly enhance its properties, producing steel. This is obtained through a variety of techniques, including carburization, quenching and tempering, practices which are also generally known as smithing (4, 26, 57). Nonetheless, the production of low-carbon iron blooms was likely intentional, as producing homogeneous, carbon-rich steel blooms suitable for smithing required advanced skill and control during smelting—abilities that were not yet fully developed in this period (58). It is therefore probable that carbon was introduced at later stages of smithing, during bloom consolidation or forging, when localized carburization could be more easily achieved under controlled workshop conditions.

Trace element analysis indicates the presence of 0.1–0.2 wt% nickel, a concentration found in Levantine ores from the Ahihud Forest, approximately 60 km north of Dor (12), suggesting a possible source. However, the association of the cargo with amphorae of Cypriot or Aegean origin (59) may also point to wider eastern Mediterranean sources.

Radiocarbon modeling of charred short-lived plant remains within the cargo, including a young oak twig embedded in slag, securely dates the blooms to the late 7th–early 6th centuries BCE. The presence of this twig, likely used for kindling, suggests furnace temperatures did not exceed ~ 1000°C (60), consistent with bloomery smelting technology.

These findings resolve a longstanding debate over the nature of Iron Age ironworking in the southern Levant. Archaeological evidence from urban sites—slag, hammer scale, and rare bloom fragments—has been variously interpreted as testimony either of smelting or smithing activities. While some scholars have argued that smelting occurred within urban centers (14, 18, 61–62), others emphasize the difficulty in distinguishing between smithing and smelting debris (14, 63).

The Dor blooms demonstrate, for the first time, that smelting and primary smithing could be spatially separated. Iron blooms could be produced in rural or remote smelting sites, transported as raw blooms, and only subsequently forged within urban centers. Indeed, all three stages of iron production—smelting, primary

smithing (bloom consolidation), and secondary smithing (artifact production)—produce diagnostic waste: slags, slag prills, and hammer scale. However, while primary smithing leaves abundant slag and prills (14, 22), secondary smithing of imported blooms would generate relatively little slag and mainly hammer scales as evidence of ironworking.

The archaeological record at Dor aligns perfectly with this model. Small-scale ironworking is attested at Dor in the 7th century BCE, evidenced by limited slag and hammer scale accumulations (22), precisely the waste expected from secondary smithing workshops. The Dor L Cargo itself reinforces this conclusion. The production of ~ 50 kg of high-quality iron blooms represented by the cargo would have generated large quantities of slag. The fact that such large-scale smelting debris is absent at Dor strongly indicates that these workshops could not have produced the iron blooms. This strengthens the case for their importation as raw material for local smithing. Thus, the Dor L cargo illustrates that slag and bloom fragments found in urban centers may primarily represent the debris of secondary smithing rather than local, primary iron production.

Trade networks

The Dor blooms also shed light on previously unknown Iron Age maritime trade in raw iron. It was long assumed that iron was not transported in the form of blooms, as the cooling of an unworked bloom was viewed as inefficient (17). Instead, it was suggested that primary smithing was typically performed by hammering the bloom while it was still hot, and that iron was usually transported and traded in the form of semi-finished or finished products, as billets (7, see above). The excavations of Khorsabad, the capital of the Neo-Assyrian Empire in the 8th century BCE, uncovered about 160 tons of iron, mostly in the shape of bipyramidal bars, and similar bars were found at Nimrud and Susa, also in Neo-Assyrian contexts. These semi- finished products were most likely hoarded as a strategic stockpile, perhaps obtained via tribute extracted by the Neo-Assyrians (4).

In contrast, the Dor Lagoon blooms suggest a parallel, possibly decentralized, system of long-distance trade operated beyond direct Neo-Assyrian control. The blooms were intentionally left unworked to facilitate their survival during maritime trade, and the primary smithing process, which would have removed this protective slag layer, was deliberately postponed, likely until after the raw material had reached its destination. This “shipping-ready” state—a raw bloom protected by its own slag—was ideal for long-distance transport. While the full extent of the Dor cargo is unknown—much of it likely salvaged in antiquity as sea levels fell (64)—the survival of these blooms points to their intentional transport as raw material. Their presence fits within Dor’s role as a Phoenician-controlled port city under shifting imperial influence.

The blooms, which are now radiocarbon dated to the late 7th–early 6th centuries BCE, were found along with basket-handle amphorae of Cypriot or Greek origin (36), known in the Levant only from post-Assyrian contexts (65). Chronologically, therefore, the cargo may correspond to a brief period of Saite-Egyptian rule between about 630 and 605 BCE. This phase followed the withdrawal of the Neo-Assyrians, which had governed Dor since approximately 733 BCE, and preceded its incorporation into the Babylonian Empire around 605 BCE. Although a short interlude, it is characterized by political revival and relative independence under strong native rulers (most notably Psammetichus I), marked by renewed centralization, foreign alliances, and a cultural renaissance drawing on earlier Egyptian traditions (66–67).

In fact, accumulating research has shown that under Egyptian domination, connections between Greece (and Cyprus) and the Levant were renewed (68–72). The establishment of East Greek trading "colonies" in Egypt during this period, most famously Naukratis on the Canopic (west) branch of the Nile (73–75), is the best-known aspect of this new Greek-Egyptian-Levantine (and most probably also Cypriot) exchange sphere. It is this maritime trade circuit that likely facilitated the arrival of Greek silver to the southern Levant (76–77). The accumulating evidence of a growing magnitude of seaborne trade in the 7th century BCE suggests that the Dor L2 cargo may have been compiled during this Egyptian interlude.

While this scenario is plausible, alternative frameworks should be considered. During the earlier phase of Neo-Assyrian rule, Dor, along with other Levantine ports, was transferred to the Phoenician king Ba'al of Tyre, as part of a vassal treaty agreement (78–80). This political arrangement stimulated a significant increase in trade, population growth, and urban development at Dor, including the construction of fortifications and a sea gate (81–83). It also remains unclear whether Dor experienced Babylonian destruction, as occurred at many other Levantine sites (84). During the Persian period, the city was granted by a Persian king—possibly Cambyses II—to Eshmun'ezer II of Sidon, as part of a political tribute (84–85).

It is also possible that the Dor cargo reflects an early example of maritime iron trade alongside commodities transported in amphorae, attested in the later Persian period. An Egyptian customs entry preserved in the Ahiqar scroll describes a large Phoenician vessel arriving in Egypt, carrying, among other items, Sidonian wine (vintage year 10) and two categories of iron (*przl*), likely referring either to the iron's origin or to different grades or types (47, 86).

To conclude, the Dor cargo may reflect activity under Egyptian rule, although Neo-Assyrian or Babylonian imperial spheres cannot be ruled out. During these periods, the port of Dor operated as a Phoenician-administered harbor under the authority of imperial client kings (36). Consequently, the iron trade represented by the Dor blooms likely took place within this Phoenician-controlled commercial framework.

Conclusion

The discovery of the Dor iron blooms fundamentally expands our understanding of both Iron Age metallurgical practice and long-distance trade in raw iron. Technologically, these finds introduce the earliest and poorly documented category of iron product—unworked blooms transported in their as-smelted, slag-encased state. Their exceptional preservation demonstrates that slag wrapping served as a protective barrier against corrosion, providing an efficient means of transport over maritime routes.

The metallurgical and contextual data firmly indicate that bloomery smelting and smithing were spatially separated processes. Iron blooms could be smelted at remote production sites, transported as raw material, and subsequently refined and forged within urban centers. This finding resolves previous debates concerning the nature of ironworking debris found in Levantine cities, demonstrating that such remains may represent secondary smithing rather than primary smelting activities.

The Dor blooms also reveal an unexpected mode of Iron Age iron trade following the Late Bronze Age collapse. Contrary to prevailing models emphasizing shipment of forged billets and bars, these blooms suggest that raw iron was actively traded across the Mediterranean, likely integrated into a broader exchange

network operating under shifting imperial authorities. The dating of the Dor cargo to the late 7th–early 6th centuries BCE may situate it within a short interlude of Saite-Egyptian control, though alternative scenarios under Neo-Assyrian or Babylonian rule remain plausible.

Finally, these findings hint at emerging long-distance trade circuits linking the Levant, Egypt, Cyprus, and the Aegean, which became increasingly prominent in the late Iron Age and early Persian period. The Dor blooms thus provide the earliest direct archaeological evidence for seaborne commerce in raw iron, transforming our understanding of Iron Age trade economies and metallurgical organization in the eastern Mediterranean.

Declarations

Competing interest:

The authors declare that they have no known competing financial interests or personal relationships that could have appeared to influence the work reported in this paper.

Funding:

This study was financed in part by a grant from the Israel Science Foundation (Grant ID 156/25 titled Iron Age Ship Cargoes from Tel Dor: Assessing Diachronic Changes in Iron Age Trade, P.I. A. Yasur-Landau) and a gift from Dr. Irwin Jacobs toward collaboration in Marine and Cyber- Archaeology between UCSD and UHaifa (P.I. T.E. Levy and A. Yasur-Landau)

Author Contribution

T.E., A.I., D.L., S.A. and A.Y.L. wrote the main manuscript text. Y.B. preserved the blooms and prepared the samples for analysis. Z.C.D. modeled radiocarbon dates. M.R. prepared the figures. T.E., T.E.L, and A.Y.L. initiated this research. T.E.L and A.Y.L. funded the study. All authors reviewed the manuscript.

Acknowledgement

We are grateful to Evgeny Strokin from the Israel Institute of Materials Manufacturing Technologies, Technion Research and Development Foundation, for assisting with the sampling of the iron bloom. We thank Mark Cavanagh of the Laboratory of Archaeobotany and Ancient Environments, Tel Aviv University, for his valuable help with the microscopic analyses. We also extend our thanks to Inbal Samet for editing the manuscript.

References

1. Hedges REM, Salter CJ. Source determination of iron currency bars through analysis of the slag inclusions. Archaeometry. 1979;21(2):161–75.
2. McDonnell JG. A model for the formation of smithing slags. Materiały Archeologiczne. 1991;26:23–6.

3. Pleiner R. Iron in Archaeology: The European Bloomery Smelters. Prague: Archeologicky Ústav AV ČR; 2000.
4. Pleiner R. Iron in Archaeology: Early European Blacksmiths. Prague: Archeologický ústav AV ČR; 2006.
5. Serneels V, Perret S. Quantification of smithing activities based on the investigation of slag and other material remains. Archaeometall Europe. 2003;1:469–78.
6. Birch T. The provenance and technology of Iron Age war booty from southern Scandinavia (Doctoral dissertation, University of Aberdeen) (2013).
7. Blakelock E, Martinon-Torres M, Veldhuijzen HA, Young T. Slag inclusions in iron objects and the quest for provenance: an experiment and a case study. J Archaeol Sci. 2009;36(8):1745–57.
8. Tylecote RF. A History of Metallurgy. London: The Metals Society; 1976.
9. Bani-Hani M, Abd-Allah R, El-Khouri L. Archaeometallurgical finds from Barsinia, northern Jordan: microstructural characterization and conservation treatment. J Cult Herit. 2012;13(3):314–25.
10. Eliyahu-Behar A, Yahalom-Mack N, Gadot Y, Finkelstein I. Iron smelting and smithing in major urban centers in Israel during the Iron Age. J Archaeol Sci. 2013;40(12):4319–30.
11. Einecke G. Die Eisenerzvorräte der Welt und der Anteil der Verbraucher-und Lieferländer an deren Verwertung. Verlag Stahleisen; 1950.
12. Rohrlich V, Metzer A, Zohar E. Potential iron ores in the Lower Cretaceous of Israel and their origin. Isr J Earth Sci. 1980;29:73–80.
13. Eliyahu-Behar A, et al. A land whose stones are iron… iron ore sources in the southern Levant. Front Environ Archaeol. 2023;2:1221130.
14. Bauvais S. Prolégomènes à une histoire de la métallurgie du fer au Levant Sud. Bull du Centre de recherche français à Jérusalem 19 (2008).
15. Erb-Satullo NL. The innovation and adoption of iron in the ancient Near East. J Archaeol Res. 2019;27:557–607.
16. Yener AK. The Domestication of Metals: The Rise of Complex Metal Industries in Anatolia. Volume 4. Brill; 2021.
17. Veldhuijzen HA, Rehren T. Slags and the city: early iron production at Tell Hammeh, Jordan, and Tel Beth-Shemesh, Israel. Met Mines Stud Archaeometall. 2007;189:201.
18. Yahalom-Mack N, et al. Metalworking at Hazor: a long-term perspective. Oxf J Archaeol. 2014;33(1):19–45.
19. Yahalom-Mack N, et al. Metalworking at Megiddo during the Late Bronze and Iron Ages. J Near East Stud. 2017;76(1):53–74.
20. Workman V, et al. An Iron IIA iron and bronze workshop in the lower city of Tell es-Safı/Gath. Tel Aviv. 2020;47(2):208–36.
21. Rothenberg B, Tylecote RF. A unique Assyrian iron smithy in the northern Negev (Israel). IAMS Newsl. 1991;17:11–4.
22. Eliyahu-Behar A, et al. An integrated approach to reconstructing primary activities from pit deposits: iron smithing and other activities at Tel Dor under Neo-Assyrian domination. J Archaeol Sci. 2008;35(11):2895–908.

23. Mascelloni ML. Testing the Evidence for Local Metalworking: Metals, Slag and Vitrified Materials from Tell Es-Sa'idiyeh, Jordan. MA thesis, Institute of Archaeology, University College London (2004).
24. Van-Horn MT. *Re-forging the Past: Interpreting Phoenician Iron Production at Tel Akko, Israel*. MA thesis, M.A. thesis, Pennsylvania State University, PA (2017).
25. López-Ruiz C. Phoenicians and the Making of the Mediterranean. Harvard University Press; 2022.
26. Snodgrass AM. Iron and Early Metallurgy in the Mediterranean. Yale University Press; 1980.
27. Aubet ME. Political and economic implications of the new Phoenician chronologies in Beyond the Homeland: Markers in Phoenician Chronology (ed. Sagona, C.) 247–259 (Peeters, 2008).
28. Kaufman B, Docter R, Fischer C, Chelbi F, Telmini BM. Ferrous metallurgy from the Bir Massouda metallurgical precinct at Phoenician and Punic Carthage and the beginning of the North African Iron Age. J Archaeol Sci. 2016;71:33–50.
29. Maeir AM. Their voice carries throughout the earth, their words to the end of the world (Ps 19, 5): thoughts on long-range trade in organics in the Bronze and Iron Age Levant, in *And in Length of Days Understanding (Job 12:12): Essays on Archaeology in the Eastern Mediterranean and beyond in Honor of Thomas E. Levy* 1 (ed. Ben-Yosef, E. & Jones, I.W.N.) 573–599Springer, (2023). https://doi.org/10.1007/978-3-031-27330-8_25
30. Sherratt S, Sherratt A. The growth of the Mediterranean economy in the early first millennium BC. World Archaeol. 1993;24(3):361–78.
31. López-Ruiz C. Phoenicians and the Making of the Mediterranean. Harvard University Press; 2022.
32. Berranger M, Fluzin P. From raw iron to semi-product: quality and circulation of materials during the Iron Age in France. Archaeometry. 2012;54(4):664–84.
33. Berranger M, et al. Technological analysis, provenance study and radiocarbon dating of iron bipyramidal semi-products of the Durrenentzen deposit (Haut-Rhin, France): a renewed vision of the iron economy during Iron Age I. ArcheoSciences Revue d'archéométrie. 2017;41(1):45–67.
34. Schwab R, et al. From Cyprus, or to Cyprus? A pilot study with osmium isotopy and siderophile trace elements to reconstruct the origin of corroded iron billets from the Kyrenia shipwreck. J Archaeol Sci Rep. 2022;42:103365.
35. Galili E, Bauvais S, Rosen B, Dillmann P. Cargoes of iron semi-products recovered from shipwrecks off the Carmel Coast, Israel. *Archaeometry* 57(3), 505–535 (2015).
36. Yasur-Landau A et al. Iron Age ship cargoes from the harbor of Dor (Israel). *Antiquity* 2025, 1–17 (2025).
37. Cronyn JM. The Elements of Archaeological Conservation. Routledge; 1990.
38. Riss D. Testing for chlorides with silver nitrate. Conserve O Gram. 1993;6(3):1–2.
39. Fahn A, Werker E, Bass P. Wood Anatomy and Identification of Trees and Shrubs from Israel and Adjacent Regions. Israel Academy of Sciences and Humanities; 1986.
40. Schweingruber FH. Anatomy of European Woods: An Atlas for the Identification of European Trees, Shrubs and Dwarf Shrubs. Paul Haupt; 1990.
41. Akkemike Ü, Yaman B. Wood Anatomy of Eastern Mediterranean Species. Verlag Kessel; 2012.
42. Crivellaro A, Schweingruber FH. Atlas of Wood, Bark and Pith Anatomy of Eastern Mediterranean Trees and Shrubs. With a Special Focus on Cyprus; Springer, 2013.

43. Manning SW, Lorentzen B, Demesticha S. Dating Mediterranean shipwrecks: the Mazotos ship, radiocarbon dating and the need for independent chronological anchors. Antiquity. 2022;96(388):968–80. https://doi.org/10.15184/aqy.2022.76.
44. Lorentzen B, Manning SW, Kahanov Y. The 1st millennium AD Mediterranean shipbuilding transition at Dor/Tantura Lagoon, Israel: dating the Dor 2001/1 shipwreck. Radiocarbon. 2014;56:667–78.
45. Manning SW, et al. A revised radiocarbon calibration curve 350–250 BCE impacts high-precision dating of the Kyrenia Ship. PLoS ONE. 2024;19(6):e0302645. https://doi.org/10.1371/journal.pone.0302645.
46. Driscoll JI, Strategic Drinking. The Archaeology of Alcohol in Early Iron Age West Central Europe. PhD dissertation, University of Wisconsin-Milwaukee, Milwaukee (2023).
47. Yardeni A. Maritime trade and royal accountancy in an erased customs account from 475 B.C.E. on the Ahiqar Scroll from Elephantine. Bull Am Schools Orient Res. 1994;293:67–78.
48. Forbes HA. Strategies and Soils: Technology, Production and Environment in the Peninsula of Methana, Greece. PhD dissertation, University of Pennsylvania, PA (1982).
49. Scott DA, Schwab R. Metallography in Archaeology and Art. Springer; 2019.
50. Van Dijk I, et al. Coupled calcium and inorganic carbon uptake suggested by magnesium and sulfur incorporation in foraminiferal calcite. Biogeosciences. 2019;16(10):2115–30.
51. Tang Y, Hailong L, Hailin Y. Magnesium geochemistry of authigenic carbonate at marine cold seep. Front Mar Sci. 2024;11:1463328.
52. Engel T, Frey W. Fuel resources for copper smelting in antiquity in selected woodlands in the Edom Highlands to the Wadi Arabah/Jordan. Flora. 1996;191(1):29–39.
53. Bronk Ramsey C. OxCal v 4.4.4. https://c14.arch.ox.ac.uk/oxcal.html (2021) (accessed 11 August 2025).
54. Reimer PJ, et al. The IntCal20 Northern Hemisphere radiocarbon age calibration curve (0–55 cal kBP). Radiocarbon. 2020;62:725–57.
55. Pleiner R. In: Pleiner R, editor. Die Wege des Eisens nach Europa in Friihes Eisen in Europa. Archeologicky Ústav AV ČR; 1981. pp. 115–28.
56. Furmanek V. Eisen während der Bronzezeit in der Slowakei. Z für Archäologie. 1988;23:183–9.
57. Güder Ü, Gates M-H, Yalçın Ü. Early iron from Kinet Höyük, Turkey: analysis of objects and evidence for smithing. Metalla. 2017;23(1):51–65.
58. Güder Ü, Mokrišová J, Verčík M, Yalçın Ü. Earliest evidence for systematic use of ultrahigh carbon steel in the ancient Aegean in the Archaic Milesia. PLoS ONE 20(3), e0312244 (2025).
59. Lehmann G, Shalvi G, Shochat H, Waiman-Barak P, Gilboa A. Iron Age II Phoenician transport-jars from a South-Levantine perspective: typology, evolution and high-resolution dating. Rivista di Studi Fenici. 2022;50:41–104. https://doi.org/10.19282/rsf.50.2022.05.
60. Kim NH, et al. Anatomy of *Quercus variabilis* charcoal manufactured at various temperatures. J Korean Wood Sci Technol. 2006;34(4):1–8.
61. Eliyahu-Behar A, et al. Iron and bronze production in Iron Age IIA Philistia: new evidence from Tell es-Safi/Gath, Israel. J Archaeol Sci. 2012;39(2):255–67.
62. Yahalom-Mack N, Eliyahu-Behar A. The transition from bronze to iron in Canaan: chronology, technology, and context. Radiocarbon. 2015;57(2):285–305.

63. Erb-Satullo NL, Walton JT. Iron and copper production at Iron Age Ashkelon: implications for the organization of Levantine metal production. J Archaeol Sci Rep. 2017;15:8–19.
64. Yasur-Landau A, et al. New relative sea-level (RSL) indications from the eastern Mediterranean: Middle Bronze Age to the Roman period (~ 3800–1800 y BP) archaeological constructions at Dor, the Carmel Coast, Israel. PLoS ONE. 2021;16(6):e0251870. https://doi.org/10.1371/journal.pone.0251870.
65. Shalvi G, Gilboa A. The long 7th century BCE at Tel Shiqmona (Israel): a high resolution chronological tool for the Levant and the Mediterranean. Levant. 2022;54(2):190–216.
66. Kahn D. The Assyrian invasions of Egypt (673–663 B.C.) and the final expulsion of the Kushites. Studien zur Altägyptischen Kultur. 2006;34:251–67.
67. Schipper BU. Egyptian imperialism after the New Kingdom: the 26th Dynasty and the southern Levant in Egypt, Canaan and Israel: History, Imperialism, Ideology and Literature (ed. Bar, S., Kahn, D. & Shirley, J. J.) 268–290 (Brill, 2011).
68. Fantalkin A. British Museum Research Publications,. Identity in the making: Greeks in the eastern Mediterranean during the Iron Age in Naukratis: Greek Diversity in Egypt; Studies on East Greek Pottery and Exchange in the Eastern Mediterranean (ed. Villing, A.) 199–208 (2006).
69. Master D. The Seaport of Ashkelon in the Seventh Century BCE: A Petrographic Study. PhD dissertation, Harvard University, Cambridge, MA (2001).
70. Master DM. Trade and politics: Ashkelon's balancing act in the seventh century BCE. Bull Am Schools Orient Res. 2003;330(1):47–64.
71. Waldbaum JC. Early Greek contacts with the southern Levant, ca. 1000–600 BC: the eastern perspective. *Bull. Am. Schools Orient. Res.* 293(1), 53–66 (1994).
72. Waldbaum JC. Seventh century BC Greek pottery from Ashkelon, Israel: an entrepot in the Southern Levant in Pont-Euxin et commerce la genèse de la route de la soie. Actes du IXe Symposium de Vani, Colchide, 1999 (ed. Faudot, M., Fraysse, A. & Geny, E.) 57–75 (Presses universitaires de Franche-Comté, 2002).
73. Fantalkin A. Naukratis as a contact zone: revealing the Lydian connection in Kulturkontakte in Antiken Welten. Vom Denkmodell zur Fallbeispiel. Proceedings des internationalen Kolloquiums aus Anlass des, 60. Geburtstages von Christoph Ulf, Innsbruck, 26. bis 30. Januar 2009 (ed. Rollinger, R. & Schnegg, K.) 27–51 (Peeters, 2014).
74. Schlotzhauer U, Villing A. East Greek pottery from Naukratis: the current state of research in Naukratis: Greek Diversity in Egypt; Studies on East Greek Pottery and Exchange in the Eastern Mediterranean (ed. Villing, A.) 53–68British Museum Research Publications, (2006).
75. Villing A, Schlotzhauer U. Naukratis and the eastern Mediterranean: past, present and future in Naukratis: Greek Diversity in Egypt; Studies on East Greek Pottery and Exchange in the Eastern Mediterranean (ed. Villing, A.) 1–10British Museum Research Publications, (2006).
76. Eshel T, Erel Y, Yahalom-Mack N, Tirosh O, Gilboa A. From Iberia to Laurion: interpreting changes in silver supply to the Levant in the late Iron Age based on lead isotope analysis. Archaeol Anthropol Sci. 2022;14(6):1–24.
77. Eshel T, Erel Y, Yahalom-Mack N, Gilboa A. One thousand years of Mediterranean silver trade to the Levant: a review and synthesis of analytical studies. J Archaeol Res. 2024;33:297–336.

78. Na’aman. N. Esarhaddon’s treaty with Baal and Assyrian provinces along the Phoenician coast. Rivista di Studi Fenici. 1994;22:3–8.
79. Na’aman. N. Was Dor the capital of an Assyrian province? Tel Aviv. 2009;36:95–109. https://doi.org/10.1179/204047809x439479.
80. Yasur-Landau A. The archaeology of maritime adaptation. In: Yasur-Landau A, Cline EH, editors. The Social Archaeology of the Levant from Prehistory to the Present. Cambridge University Press; 2019. pp. 551–70. & Rowan Y. M.).
81. Gilboa A, Sharon I. The Assyrian karu at Du’ru/Dor in *The Provincial Archaeology of the Assyrian Empire* (ed. Macginnis, J., Wicke, D., Greenfield, T. & Stone, A.) 241–252McDonald Institute for Archaeological Research, (2016).
82. Arkin Shalev E, Gilboa A, Yasur-Landau A. The Iron Age maritime interface at the South Bay of Tel Dor: results from the 2016 and 2017 excavation seasons. Int J Nautical Archaeol. 2019;48(2):439–52.
83. Arkin Shalev E, Galili E, Waiman-Barak P. Yasur-Landau, A. Rethinking the Iron Age Carmel Coast: a coastal and maritime perspective. Isr Explor J. 2021;71(2):129–61.
84. Stern E, Dor. Ruler of the Seas: Twelve Years of Excavations at the Israelite-Phoenician Harbor Town on the Carmel Coast. Israel Exploration Society; 1994.
85. Elayi J. An updated chronology of the reigns of Phoenician kings during the Persian period (539–333 BCE). *Transeuphratène* 32, 11–43 (2006).
86. Tal O. On the identification of the ships of KZD/RY in the erased customs account from Elephantine. J Near East Stud. 2009;68(1):1–8.

Figures

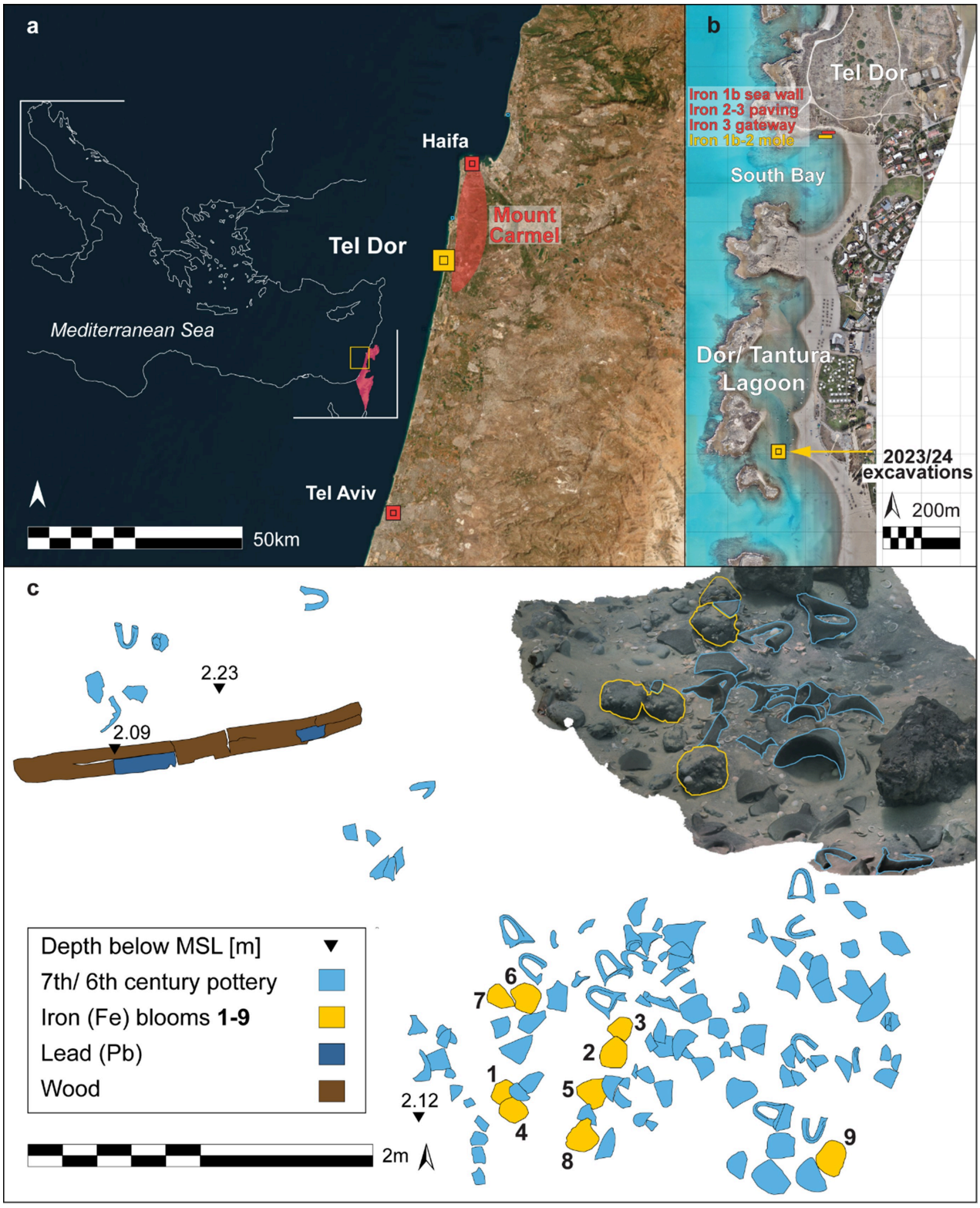

Figure 1

Maps showing the location of Dor/Tantura Lagoon and 7th–6th centuries cargo: (a) Dor in the Levant; (b) Tel Dor and its Iron Age harbour remains (see 82), including the location of the 2023–2024 expeditions; (c) top plan showing iron Blooms 1–9 in context with pieces of basket-handle amphorae and wooden anchor stock to the north. To the right, orthographic 3-D model from 2023 expedition showing five iron blooms (map a: Earthstar Geographis, generated with ArcGIS Pro; aerial b: A. Tamberino; 3-D model and figure by M. Runjajić).

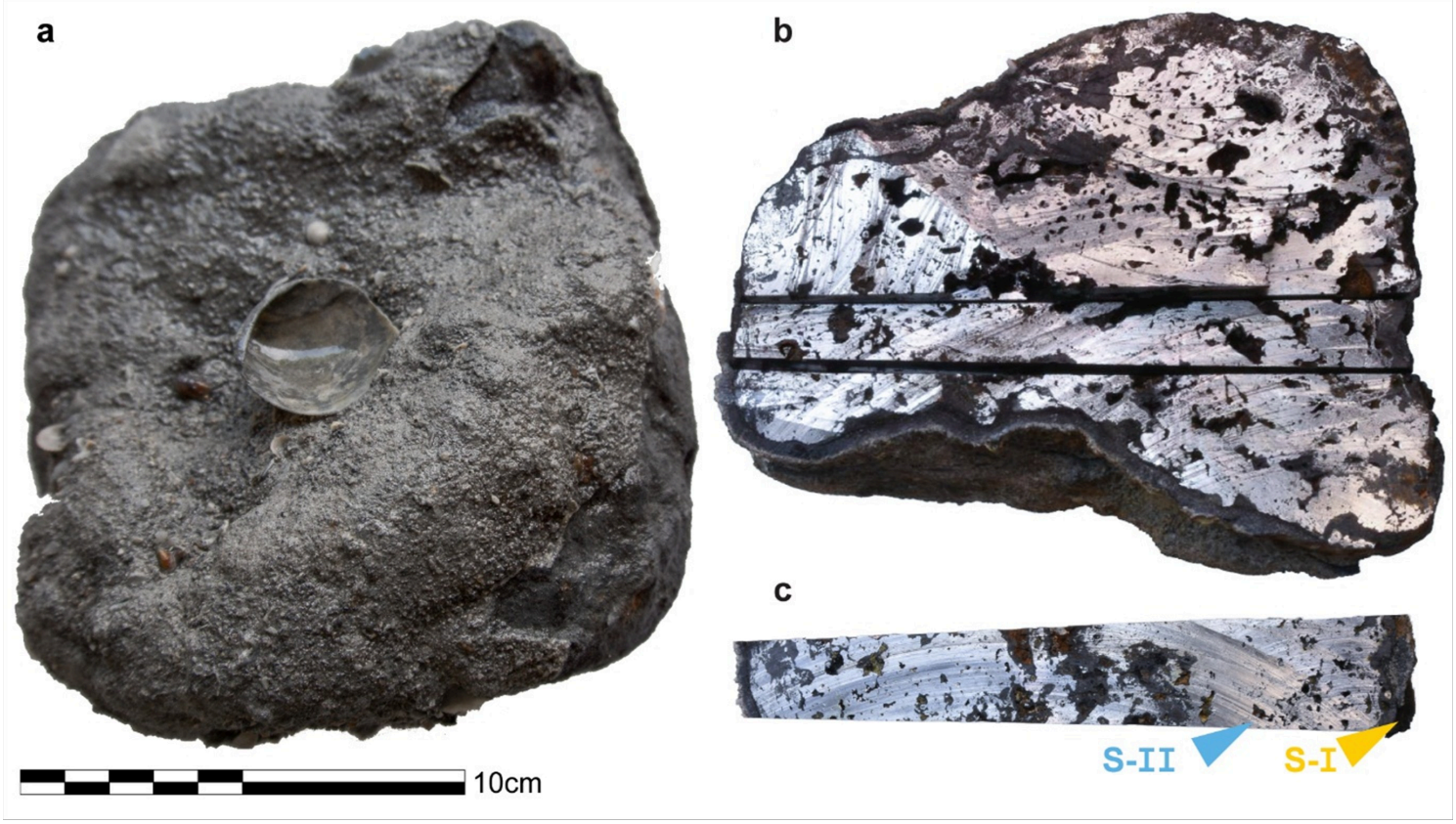

Figure 2

The iron bloom (a) after cutting a cross-section from its core; arrows point to object's crust. (b) location of metallographic samples from the cross-sections are marked S-I and S-II.

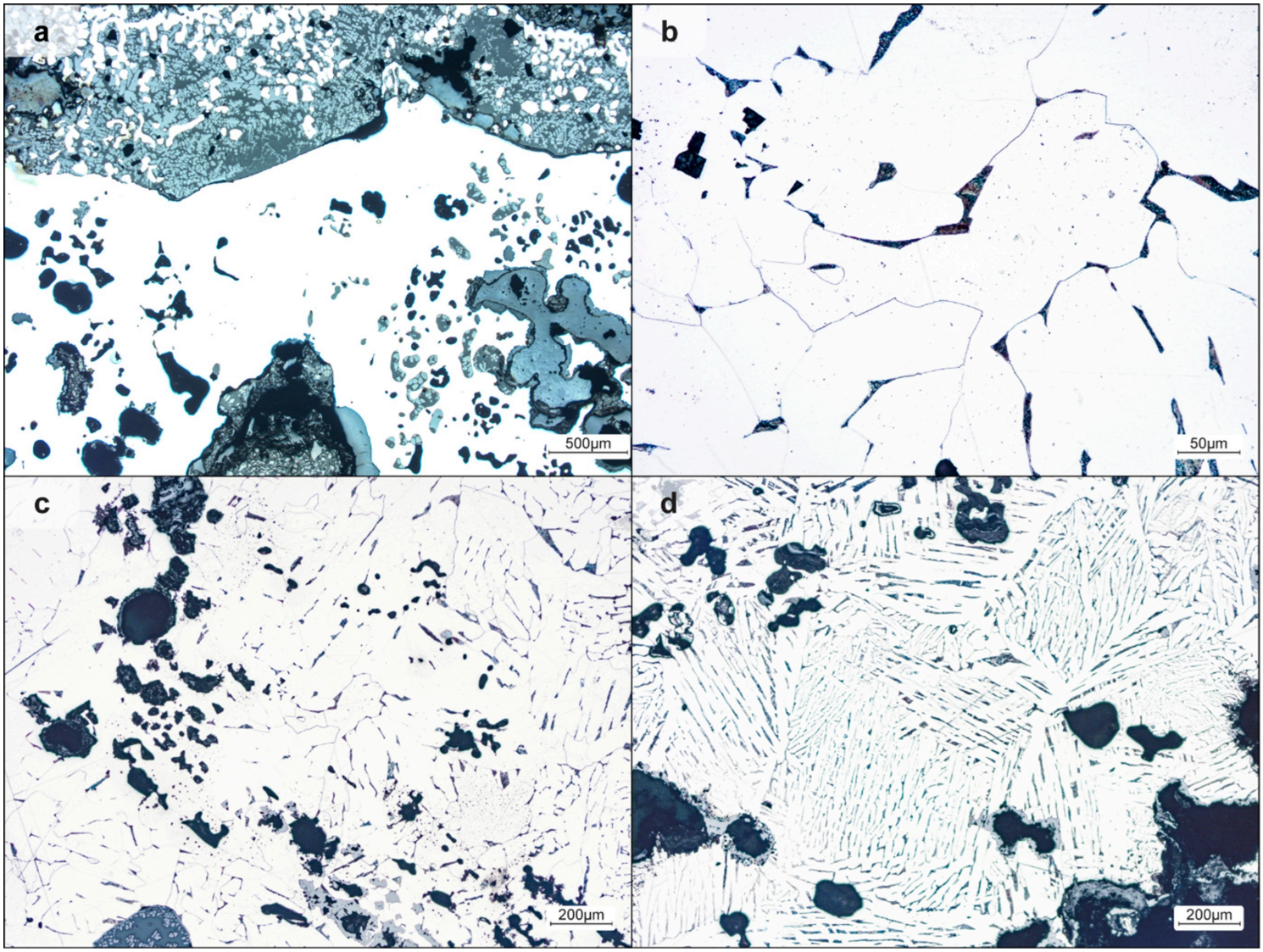

Figure 3

(a) Sample S-I: slag crust and pores near surface; OM, unetched. (b) Sample S-II: microstructure of area with low pearlite content; OM, etched. (c) Sample S-II: area with higher pearlite content; OM, etched. (d). Sample S-II: The Widemanstätten structures indicate relatively rapid cooling; OM, etched.

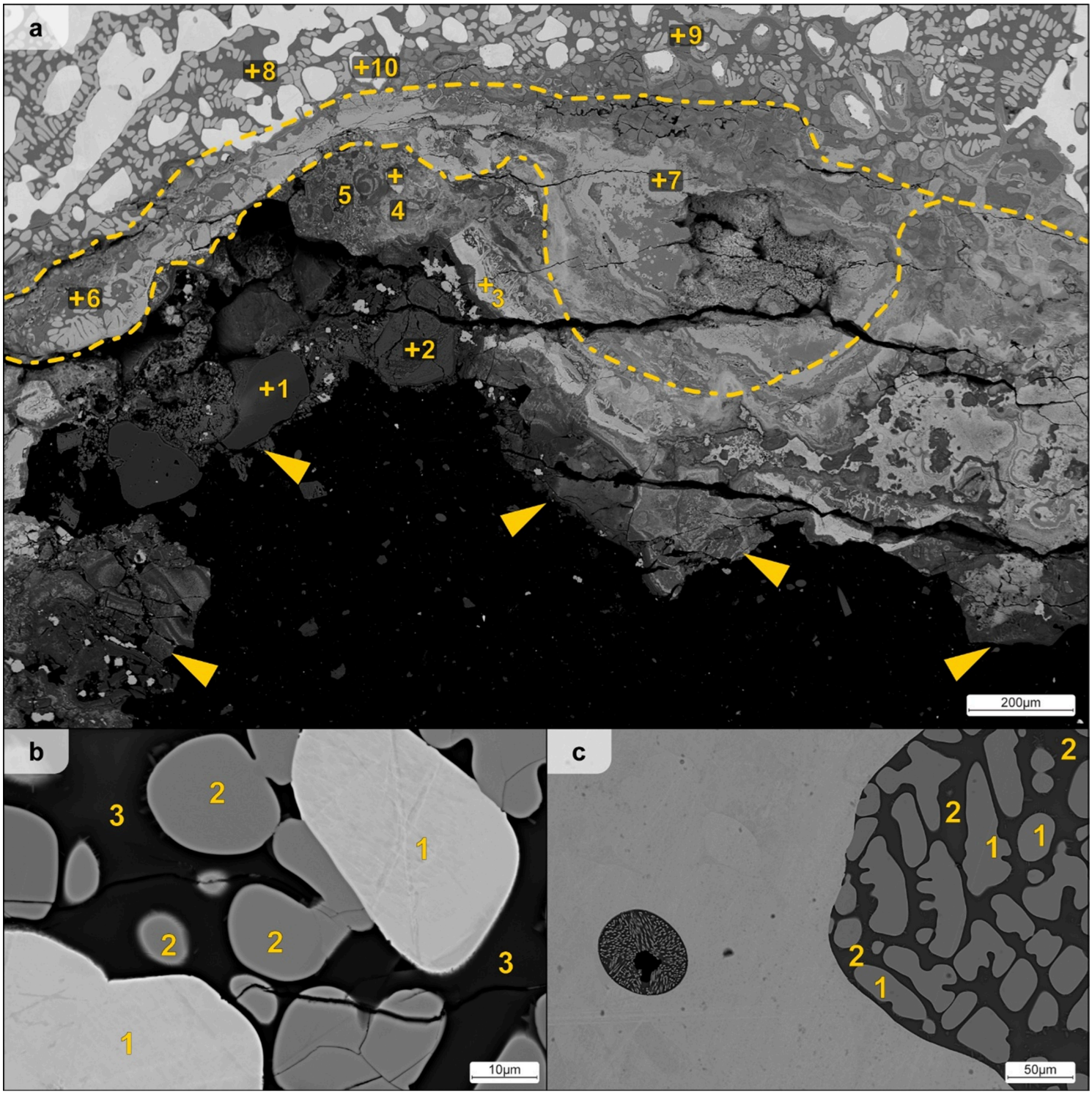

Figure 4

SEM images. For chemical composition, see Table 1. (a) Sample S-I: crust microstructure; arrows show the surface that was exposed to seawater. Numbers represent different points of analysis: 1 = sand particles; 2 = Ca-containing sediments; 3, 4 = sulfides;5 = Mg-containing sediments; 6, 7 = iron-containing corrosion products; 8 = glassy slag; 9 = iron oxides in slag; 10 = iron particles in slag. The iron-containing corrosion-products phase was identified (locations 6 and 7, framed). (b) Sample S-I: microstructure of the slag on the bloom surface. Numbers represent different points of analysis: 1 = iron particles, 2 = FeO particles, 3 = glassy

slag. (c) Sample S-II: a slag inclusion in the bulk of the iron bloom. Numbers represent different points of analysis.

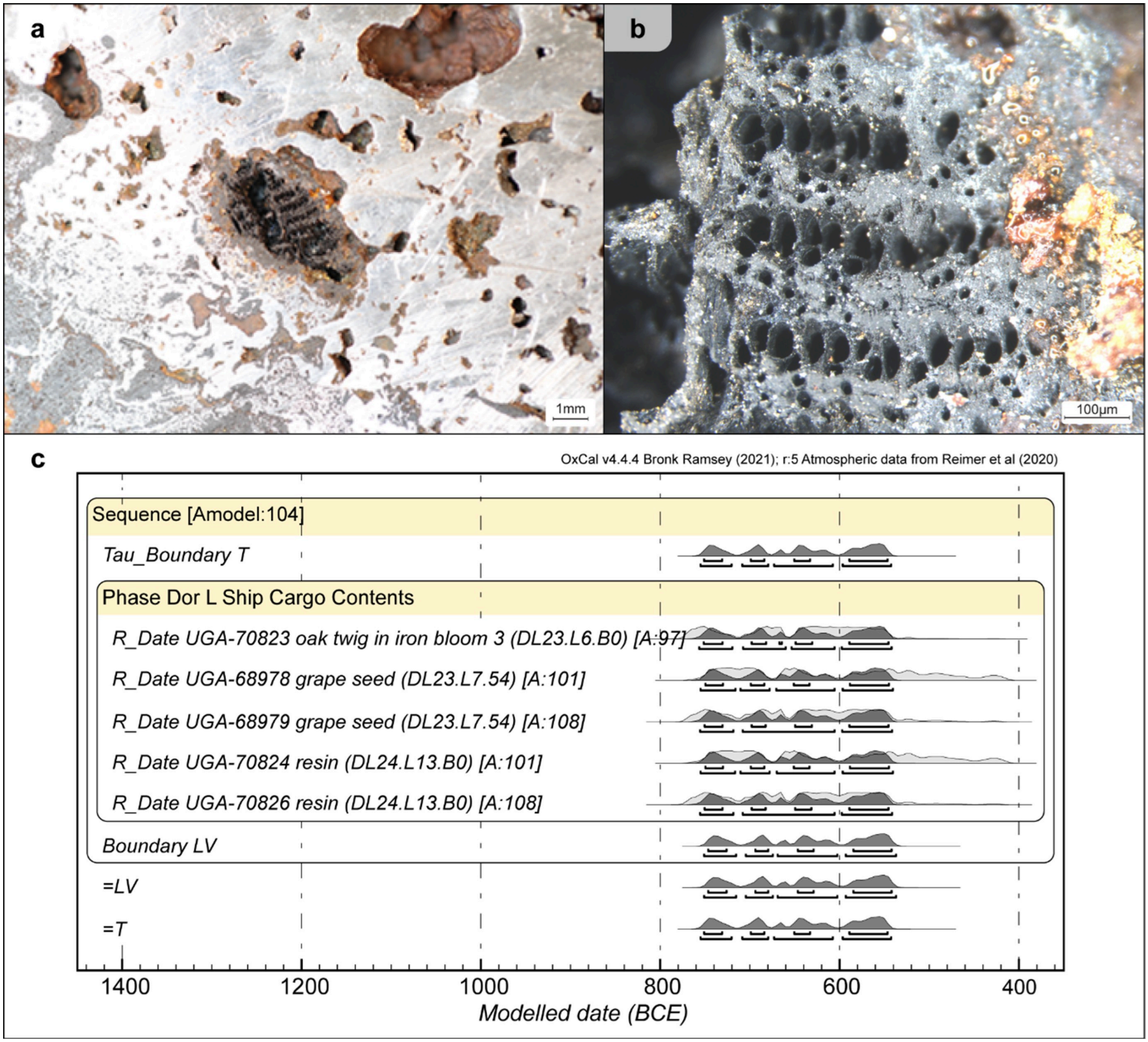

Figure 5

(a) Piece of charcoal trapped in the ingot; (b) Transverse view of charcoal fragment, identified as Quercus sp. (deciduous oak likely belonging to the Quercus subsp. quercus group; see more in SI and Fig. S3). (c) Radiocarbon modeling of an embedded young charred oak twig, together with additional short-lived (last voyage) carbon samples from the Dor L2 Cargo. The results date the blooms to the late 7th to early 6th centuries BCE.

Supplementary Files

This is a list of supplementary files associated with this preprint. Click to download.

- SIEsheletalIronBlooms.pdf